Structure and thermodynamics of colloid-polymer mixtures: A macromolecular approach

M. Fuchs[1] and K. S. Schweizer[2]

[1] *Physik-Department, Technische Universität München - 85747 Garching, Germany*
[2] *Departments of Materials Science & Engineering and Chemistry, University of Illinois Urbana, IL 61801, USA*

Abstract. – The change of the structure of concentrated colloidal suspensions upon addition of non-adsorbing polymer is studied within a two-component, Ornstein-Zernicke–based liquid state approach. The polymers' conformational degrees of freedom are considered and excluded volume is enforced at the segment level. The polymer correlation hole, depletion layer, and excess chemical potentials are described in agreement with polymer physics theory in contrast to models treating the macromolecules as effective spheres. Known depletion attraction effects are recovered for low particle density, while at higher densities novel many-body effects emerge which become dominant for large polymers.

Colloid-polymer mixtures (CPM) play an important role among dispersion systems for quite different reasons. On the one hand, their technological use has long been realized and the specific colloid-colloid interaction caused by free polymer, the depletion attraction [1,2], is exploited to induce flocculation or phase separation in dispersions. On the other hand, this system allows one to experimentally address the fundamental question about the requirements on the pair potential for a liquid phase to exist [2,3]. For even more complex systems CPM serves as a model system in order to address protein crystallization [4,5] and other phenomena involving spherical nanoparticles.

Recent field-theoretic considerations of a few colloidal particles in dilute polymer solutions [6], and scaling arguments for semidilute solutions [7], have clarified the polymer structure close to particles and provided a fundamental understanding of the origins of the depletion attraction. The phase diagram of sterically stabilized hard-sphere–like colloidal particles in polymer solutions close to their Θ-point has been mapped out in detail [3], and a rather successful mean-field–like theory for it exists [8]. The thermodynamic approach of Lekkerkerker *et al.* maps the CPM onto a binary hard-sphere mixture with *non*-additive radii, allowing the effective polymer spheres (EPS) to overlap, but excluding them from the colloids. Simulation studies for a closely related model support some of the theoretical predictions [9].

So far little, however, is known about the structure of the CPM, nor how depletion phenomena change when particles are small compared to polymers. Whereas neutron scattering

experiments [10] on rather low-density colloids could be fit into an effective pair potential description, more recent light scattering experiments on more concentrated systems [11] have evaded theoretical explanations with EPS models [12], and the assumption of a colloid structure unperturbed by polymer fails [8, 11]. Removing the assumption of an unaffected local colloid structure forces one to develop a new approach to CPM which explicitly addresses local structure. Moreover, as the packing of polymers into the void space between particles is of intrinsic interest on its own, a microscopic two-component approach appears desirable and shall be presented in this letter. This macromolecular approach further provides the unique possibility to explore the full range of colloid-polymer size ratios.

We consider a two-component system consisting of hard spheres of diameter σ_c at packing fraction $\phi_c = \frac{\pi}{6}\varrho_c\sigma_c^3$, and polymers modeled as chains of segments (excluded-volume diameter σ_p) characterized by a (Padé-approximated) Gaussian intramolecular structure factor $\omega(q)$ [13], where q is the wave vector. In matrix notation, with a diagonal matrix of intramolecular structure factors ($\hat{\omega}_{11} = \omega(q)$, and $\hat{\omega}_{22} = 1$), diagonal matrix of site number densities, ϱ_{ij}, and a matrix of direct, $\hat{c}_{ij}(q)$, and intermolecular, $\hat{h}_{ij}(q)$, site-site correlation functions, the Ornstein-Zernicke–like equations for the total structure factors, $\hat{S}_{ij}(q)$, are [13,14]

$$\hat{S}^{-1}(q) = [\varrho\hat{\omega}(q) + \varrho\hat{h}(q)\varrho]^{-1} = \hat{\omega}^{-1}\varrho^{-1} - \hat{c}(q) . \tag{1}$$

Together with the constraints of (additive) local steric exclusion, $g_{ij}(r < \frac{1}{2}(\sigma_i + \sigma_j)) = 0$, where the $g_{ij}(r) = 1 + h_{ij}(r)$ are the intermolecular pair correlation functions, eq. (1) may be viewed as a definition of the effective interactions $c_{ij}(r)$. For the pure colloid component we adopt the well-established Percus-Yevick (PY) approximation, $c_{cc}(r > \sigma_c) = 0$. For the pure athermal polymer component, the polymer reference interaction site model (PRISM) approach is employed as it has proved versatile and successful for polymers [13,14]. PRISM considers the segment averaged polymer structure and, in the most simple version, adopts a PY-like closure, $c_{pp}(r > \sigma_p) = 0$ [13,14], also derivable from a Gaussian field-theoretic perspective [15].

To close the integral equations, a further approximation for the colloid-polymer direct correlation function is required. We propose a novel generalization of the PY closure motivated by the known physical behavior of polymer packing near a spherical particle [6]:

$$\hat{c}_{cp}(q) = \frac{\hat{c}_{cp}^s(q)}{1 + q^2\lambda^2} , \quad \text{with} \quad c_{cp}^s(r > \frac{\sigma_c + \sigma_p}{2}) = 0 . \tag{2}$$

On the segmental level, again the central idea of a short-ranged steric interaction is used, and leads to the expectation that $c_{cp}^s(r)$ is repulsive and varies rapidly for $r \lesssim \frac{\sigma_c + \sigma_p}{2}$. But additionally, an effective entropic repulsion between segments and particle is present over a length scale λ beyond contact due to chain connectivity constraints. On physical grounds λ cannot be larger than the smaller of the two sizes (colloid or polymer). In general, the nonlocality length λ will depend on the densities and relative sizes, and additional information is required to determine it. We use the argument of thermodynamic consistency and calculate the excess free energy of insertion per segment of a polymer coil into the pure colloidal hard-sphere solution via two independent routes [14]. From the compressibility route of concentrating the colloid solution around the polymer ($\beta = 1/k_\mathrm{B}T$):

$$\beta\delta\mu_p^{(c)}|_{\varrho_p=0} = -\int_0^{\varrho_c} \mathrm{d}\varrho_c' \, \hat{c}_{cp}(q = 0, \varrho_c') , \tag{3}$$

and from the charging route which considers the free energy required to grow the particles
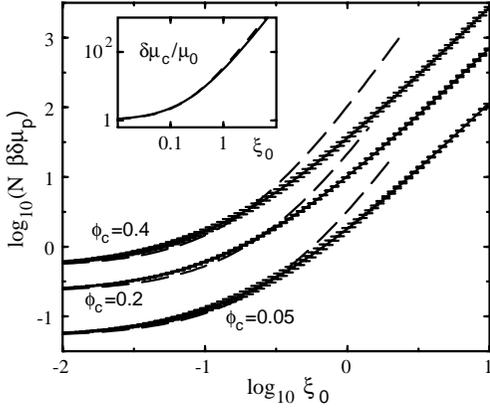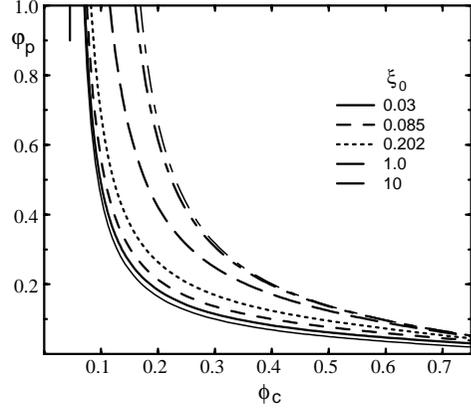
Fig. 1

Fig. 2

Fig. 1 – Excess chemical potential $N\beta\delta\mu_p^{(c)}|_{\varrho_p=0}$ for inserting one polymer into a hard-sphere fluid *vs.* polymer size for three colloid packing fractions. The present results, where error bars mark the differences from eqs. (3), (4), are compared to the equivalent PY results for inserting a sphere of radius equal to R_g (dashed lines) as used in the phantom sphere approach of ref. [8]. The inset compares the excess free energy cost (solid line from eq. (5) where $\mu_0 = \frac{\pi}{6}c_p\sigma_c^3/\beta$) for adding one colloidal sphere to a dilute polymer solution as a function of relative polymer size, $\xi_0 = R_g/(\sqrt{2}\sigma_c)$, with the field-theoretic result, dashed line [6].

Fig. 2 – Spinodal curves for various size ratios. The polymer-size–independent asymptote $\phi_c \to 1/22$ for $\varphi_p \to \infty$ is marked by a vertical bar. The limits for small or large polymer sizes are included as thin solid or dot-dashed line, respectively.

from points to their actual sizes:

$$\beta\delta\mu_p^{(g)}|_{\varrho_p=0} = \frac{\pi\varrho_c\sigma_c}{2}\int_0^1 d\zeta(\sigma_p+\zeta\sigma_c)^2 g_{cp}^{(\zeta)}(\frac{\sigma_p+\zeta\sigma_c}{2}) + 2\pi\varrho_c^2\sigma_c\int_0^1 d\zeta(\sigma_p+\zeta\sigma_c)^2 \frac{\partial g_{cc}^{(\zeta)}(\zeta\sigma_c)}{\partial\varrho_p}\bigg|_{\varrho_p=0} .(4)$$

Equating the excess free energies from both routes determines λ, and, as we first focus on dilute polymer solutions, determining it at $\varrho_p = 0$ appears justified. As a technical approximation we analytically determine the leading limiting behaviors and match the following Padé-form to λ: $\lambda^{-1} = \xi^{-1} + \frac{1+2\phi_c}{1-\phi_c}\frac{\lambda_1}{\sigma_c}$, where $\lambda_1 = (\sqrt{5}+1)$. Here ξ is the (collective) polymer correlation length and determines the width of the depletion layer in the large particle limit [7,13]. For accessible colloid densities and size ratios, the different routes, eqs. (3), (4), to the insertion free energies at vanishing polymer concentration then agree with relative errors smaller than 15%. Representative results are shown in fig. 1. Using the results for ξ from eqs. (1) to (4) at finite polymer concentrations provides a reasonable approximation to the exact λ at all densities. The chemical potential to add single colloidal spheres to a polymer solution from the compressibility and free energy routes then agrees within an error of a factor 3 at most.

The aspect of a large length scale separation, $\sigma_c/\sigma_p \approx 10^3$, thwarts numerical studies of many realistic systems, but can be exploited in a scaling limit of shrinking the polymer segment size, σ_p, to zero; for a rigorous derivation of this field theory inspired "thread-limit" of PRISM for Gaussian chains see [16]. Then the system is characterized by the colloid packing fraction, ϕ_c, the reduced polymer concentration, $\varphi_p = 2\pi c_p\xi_0^3$, where c_p is the polymer-molecule number density, and the polymer size $\xi_0 = R_g/\sqrt{2}$, where R_g is the radius of gyration. Note that we

now use the colloid diameter as unit of length; $\sigma_c = 1$. Flexible Gaussian polymers are obtained where the statistical segment size $\sqrt{6}\sigma_p$ follows from eqs. (3), (4) for $\varrho_p \to 0$ and $\varrho_c \to 0$. The effective polymer concentration, $\varphi_p \propto c_p/c_p^*$, is measured relative to the dilute-semidilute crossover concentration, c_p^*, where the polymer coils start to overlap. This first result from the present macromolecular approach justifies EPS models, where $\eta_p = \frac{4\pi}{3}c_p R_g^3 \approx \varphi_p/0.53$ is used from the outset. For $\phi_c = 0$, the polymer correlation length is $\xi = \xi_0/(1+2\varphi_p)$ [13]. The connection of the thread limit of PRISM to Gaussian field theory and scaling approaches has been discussed [13,15].

The non-linear integral equations can now be solved with the Wiener-Hopf factorization technique; details will be presented elsewhere. The lines of spinodal instabilities, where the (partial) compressibilities diverge indicating fluid-fluid phase separation, can be found accurately without the need of extrapolations of numerical integration schemes. In fig. 2, one observes the trend that the required dimensionless polymer density increases as R_g grows and/or particle diameter decreases. This prediction [17] is in qualitative agreement with many experiments on polymer-colloid, protein or micelle suspensions [3,18], but in disagreement with EPS models which do not account for polymer-polymer repulsive interactions, many body depletion effects, nor particle penetration of polymer coils, all of which tend to reduce the tendency for phase separation.

The polymer segment profile close to a colloidal particle is correctly predicted to be of a parabolic form: $g_{cp}(r) \dot{=} \frac{A}{\lambda\xi}(r - \sigma_c/2)^2 + \ldots$, where $A \to \frac{1}{2} + (\lambda+\xi)/\sigma_c$ for $\phi_c \to 0$. For nonzero λ, and simplifying to small polymers, $\xi_0 \ll \sigma_c$, the number of polymer segments in contact with the colloid particle is of order unity for a single polymer and becomes independent of the polymer degree of polymerization in the semidilute regime, $\varrho_p g_{cp}(r \approx \frac{\sigma_c+\sigma_p}{2}) \propto c_p(1+2\varphi_p)^2 \to (\varrho_p\sigma_p^3)^3$. This behavior is in agreement with scaling [7] considerations. Quantitatively we find good agreement as $\varphi_p \to 0$: $A \to 1/2$ or $A \to \frac{\xi_0}{\sigma_c}$ for $\xi_0 \to 0$ or $\xi_0 \to \infty$, respectively, compared to $A \to 1/2$ or $A \to 4\frac{\xi_0}{\lambda_1\sigma_c}$ from field theory for a single Gaussian chain [6]. For the PY closure, where $\lambda = 0$, this behavior is violated and thus the polymer-induced depletion attraction is significantly underestimated [19]. The free energy of insertion of a sphere into a polymer solution can be obtained from the free energy route (analog of eq. (4)) as

$$\beta\delta\mu_c^{(g)}|_{\varrho_c=0} = \frac{\pi c_p \sigma_c^3 \xi_0^2}{6\xi^2}\left(1 + \left(6 + \frac{3}{2}\lambda_1\right)\left(\frac{\xi}{\sigma_c}\right) + 6\lambda_1\left(\frac{\xi}{\sigma_c}\right)^2\right). \tag{5}$$

For dilute polymer solutions, eq. (5) is compared with field-theoretic calculations [6] in the inset of fig. 1, and excellent agreement is found. Whereas the colloid excess chemical potential measures the number of excluded polymer molecules for small coils, for large polymers, $\xi \gg \sigma_c$, only segments along a strand of length proportional to the colloid size need to be rearranged, and the result becomes intrinsic (independent of polymer size), $\beta\delta\mu_c|_{\varrho_c=0} \propto \varrho_p\sigma_c\sigma_p^2$. For identical physical reasons as in eq. (5), the chemical potential for inserting a large polymer into a sphere fluid becomes intrinsic, $\beta\delta\mu_p|_{\varrho_p=0} \propto R_g^{1/\nu}/N \propto N^0$ with $\nu = \frac{1}{2}$, as the small spheres need to accommodate $\mathcal{O}(R_g^{1/\nu})$ polymer segments. This asymptotic behavior is apparent in fig. 1 and qualitatively agrees with RISM-based theory for a single delocalized electron in a hard-sphere fluid [20]. EPS models, which predict $\beta\delta\mu_p|_{\varrho_p=0} \propto R_g^3/N \propto N^{1/2}$ [8], already begin to deviate from PRISM for $\xi_0 < \sigma_c$, as seen in fig. 1. This N-dependent overestimate of the polymer insertion chemical potential has direct consequences on the predicted trends for phase separation as a function of ξ_0/σ_c, which are opposite to our results in fig. 2.

Figure 3 shows the pair correlation functions for different parameter sets with increasing colloid concentrations. For rather short polymers, fig. 3(a), the polymer-induced depletion attraction leads to a strong increase of the colloid contact value, $g_{cc}(r = \sigma_c+)$, relative to the
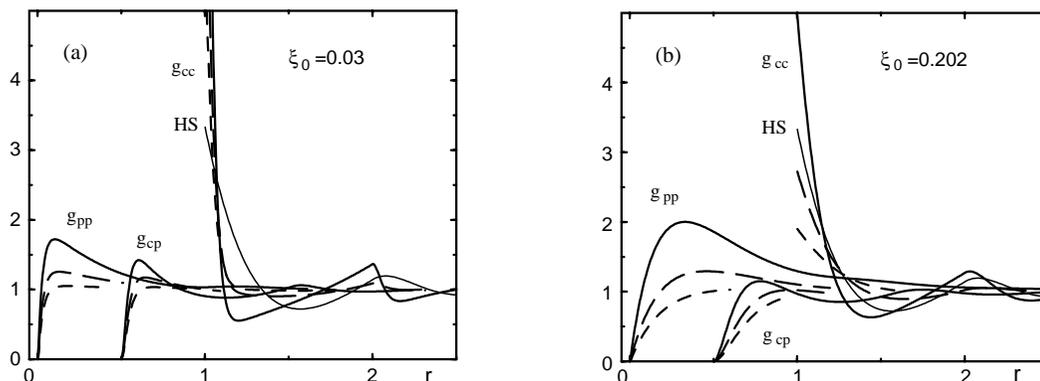
Fig. 3 – Pair correlation functions for two polymer sizes ξ_0. In (a), $\xi_0 = 0.03$ and reduced polymer concentration $\varphi_p = 0.061$, for increasing colloid packing fractions, $\phi_c = 0.05$, 0.2 and 0.4; $g_{cc}(r)$ increases to the contact values of $5.80, 8.11$ and 14.1. In (b), $\xi_0 = 0.202$ and identical ϕ_c are shown at $\varphi_p = 0.086$. For both polymer sizes the small-q limit of the colloid structure factor agrees at $\phi_c = 0.40$, where $S_{cc}(q = 0)/\varrho_c = 0.80$. The thin solid lines in both panels labeled HS give the PY-result for hard spheres at $\phi_c = 0.40$.

hard-sphere value. The polymer depletion layer is visible in $g_{cp}(r)$ for $r - \frac{1}{2} < \xi$. Outside of the depletion region oscillatory correlations are found at higher ϕ_c reflecting the imprinting of colloid order on segment-particle packing. Clustering results in the interchain polymer segment correlations, $g_{pp}(r)$, and fills the correlation hole, which in pure dense polymer fluids results from effective intermolecular repulsions extending out to ξ_0 [13]. As the polymer correlations may be considered to decay for $r \leq \sigma_c$, the description of the colloid structure when $\sigma_c \gg \xi_0$ appears amenable to traditional one-component effective pair potential approaches [1,2], which rely on the assumption of negligible long-ranged polymer correlations.

For larger polymers the depletion layer in fig. 3(b) widens as expected. Moreover, increasing colloid volume fraction leads to much longer-ranged polymer fluctuations as strikingly apparent for g_{pp} at $\phi_c = 0.40$. The clustering enforced by the void structure among the colloidal spheres overwhelms the polymer repulsion responsible for the correlation hole. As the polymer correlations extend beyond a number of particle diameters, effective pair potentials cannot be used. Three- and higher-body contributions to the effective colloid interactions become important which are mediated by the increasingly correlated polymer structure; this is in qualitative agreement with simulation studies of a simplified model using interpenetrating polymers [9], which should apply to our systems for low polymer concentrations (fugacities). The small (large) change of the local structure in g_{cc} for large (small) polymers, respectively, is also seen in these simulations. Our results at higher polymer concentrations further show that the polymer-induced depletion attraction is decreased by polymer-polymer excluded-volume interactions as has been observed in neutron scattering experiments [10].

The structure of the colloidal liquid at triple coexistence has been the focus of a recent light scattering study which determined $S_{cc}(q)$ for $1.4 \leq q\sigma_c \leq 7.2$ [11]. Figure 4 shows the data and theoretical curves evaluated without adjustable parameter. The small-q colloid structure shows a strong dependence on polymer size. The theory accurately predicts the long-wavelength fluctuations which correspond to an order of magnitude enhancement of the osmotic compressibility relative to pure hard spheres. The large-angle colloid structure experimentally shows little discernible polymer size dependence. The theory correctly captures
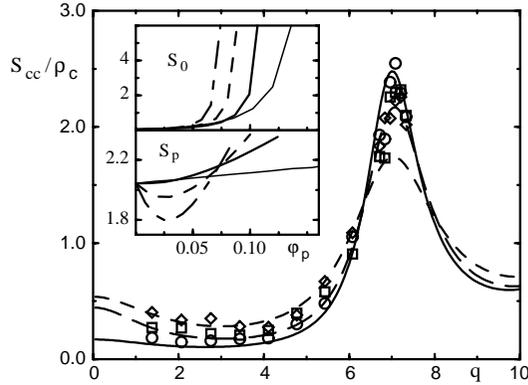
Fig. 4 – Colloid structure factors compared to the experimental data by Moussaid *et al.* [11]. The parameters are $(\phi_c, \varphi_p, \xi_0) = (0.333, 0.069, 0.085;$ short dashes and $\diamond)$, $(0.404, 0.069, 0.131;$ long dashes and $\square)$, and $(0.444, 0.053, 0.202;$ solid line and $\circ)$. The inset shows the reduced polymer concentration dependence of the colloid structure factors at the peak $S_p = S_{cc}(q_p)/\varrho_c$, and at small wave vectors, $S_0 = S_{cc}(0)/\varrho_c$, at fixed colloid packing fraction, $\phi_c = 0.40$, and for increasing polymer sizes, $\xi_0 = 0.03$ (dot-dashed), 0.085 (short dashed), 0.202 (solid), and 1 (thin solid line).

the large-q trend concerning the peak intensity and location, except for the smallest polymer where a decrease in the peak height larger than seen in the experiments is predicted. The insets in fig. 4 contrast the different trends of the colloid structure at small and large wave vectors when changing the polymer concentration for different polymer sizes. Whereas, the colloidal osmotic compressibility, $S_{cc}(q = 0)/\varrho_c$, increases mainly due to approaching the spinodal, non-monotonic variations in the large angle scattering peak height, $S_{cc}(q_p)$, arise for small polymers corresponding to a polymer-mediated distortion of the local collective packing ("cage") around a particle. Based on dynamic mode coupling ideas [21], we expect this effect to cause the melting of the colloidal glass upon addition of small amounts of small polymer ($\xi_0 = 0.03$) as reported in [3].

In the limit where the spheres act as small depletants for the larger polymers, the description of the intermolecular structure functions simplifies. Except for corrections of $\mathcal{O}(\sigma_c/\xi_0)$, the packing of the colloids becomes hard-sphere–like. The polymer segment-segment pair correlation function becomes long ranged:

$$g_{pp}(r) \rightarrow 1 + \tfrac{\xi_0}{2\varphi_p r}(e^{-\frac{r}{\xi_*}} - e^{-\frac{r}{\xi_0}}) \qquad \text{for } \xi_0 \gg \sigma_c , \tag{6}$$

where the collective correlation length ξ_*, with $\xi_0/\xi_* = 1 + 2\varphi_p(1 - f_\infty(\phi_c))$, describes the decay of the polymer density from its (intermolecular) contact value, $f_\infty(\phi_c) = \frac{\phi_c(6\lambda_1 + 1 - 4\phi_c)}{2(1 - \phi_c)(1 + 2\phi_c)}$, to zero. Polymer phase separation can be brought about by increasing the colloid density, as a spinodal instability ($1/\xi_* = 0$) exists. This phase separation requires finite polymer concentrations, leads to a dense phase of interpenetrating polymers, and results from the increased intermolecular attraction induced by the spherical depletants.

To summarize, building upon the successful description of the structure of hard-spheres and athermal polymer solutions, we have developed a microscopic theory of the thermodynamics and structural correlations of binary particle-polymer mixtures. The inclusion of many-body interaction effects proves crucial for a successful description of the CPM-structures at higher densities. The explicit consideration of the conformational entropic contributions of the polymers is required to address the packing of larger polymers into the void space between

colloidal spheres. Whereas solely entropic (steric) effects are considered here, extensions to include temperature-dependent solvent quality effects and attractions have been achieved for dilute systems [22], and can in principle also be incorporated for finite concentrations.

<center>* * *</center>

REFERENCES

[1] Asakura A. and Oosawa F., *J. Chem. Phys.*, **22** (1954) 1255; *J. Polym. Sci.*, **33** (1958) 183.
[2] Gast A. P., Hall C. K. and Russel W. B., *J. Colloid Interface Sci.*, **96** (1983) 251.
[3] Ilett S. M., Orock A., Poon W. C. K. and Pusey P. N., *Phys. Rev. E*, **51** (1995) 1344.
[4] Rosenbaum D., Zamora P. C. and Zukoski C. F., *Phys. Rev. Lett.*, **76** (1996) 150.
[5] Poon W. C. K., *Phys. Rev. E*, **55** (1997) 3762.
[6] Eisenriegler E., Hanke A. and Dietrich S., *Phys. Rev. E*, **54** (1996) 1134.
[7] Joanny J.-F., Leibler L. and de Gennes P. G., *J. Polymer Sci.: Polymer Physics*, **17** (1979) 1073.
[8] Lekkerkerker H. N. W., Poon W. C. K., Pusey P. N., Stroobants A. and Warren P. B., *Europhys. Lett*, **20** (1992) 559.
[9] Meijer E. J. and Frenkel D., *J. Chem. Phys.*, **100** (1994) 6873; *Phys. Rev. Lett.*, **67** (1991) 1110; *Physica A*, **213** (1995) 130.
[10] Ye X., Narayanan T., Tong P. and Huang J. S., *Phys. Rev. Lett.*, **76** (1996) 4640.
[11] Moussaïd A., Poon W.C.K., Pusey P.N. and Soliva M.F., *Phys. Rev. Lett.*, **82** (1999) 225.
[12] Louis A. A., Finken R. and Hansen J.-P., *Europhys. Lett.*, **46** (1999) 741; Dijkstra M., Brader J. M. and Evans R., *J. Phys. Condens. Matter*, **11** (1999) 10079.
[13] Schweizer K. S. and Curro J. G., *Adv. Chem. Phys*, **98** (1997) 1.
[14] Chandler D., *Studies in Statistical Mechanics*, edited by Montroll E. W. and Lebowitz J. L., Vol. **VIII** (North-Holland, Amsterdam) 1982, p. 274.
[15] Chandler D., *Phys. Rev. E*, **48** (1993) 2898.
[16] Fuchs M., *Z. Phys. B*, **103** (1997) 521.
[17] In the limit, $\phi_c \to 0$, $\sigma_c \gg \xi_0$ the depletion attraction becomes much larger than $k_B T$ even if $\varphi_p \ll 1$, [1,7]. In this regime, many particle approaches, both classic [2,8] and liquid state theory [19], underestimate the attraction. Our spinodal curves become less reliable there.
[18] See for example: Verhaegh N. A. M., van Duijneveldt J. S., Dhont J. K. G. and Lekkerkerker H. N. W., *Physica A*, **230** (1996) 409; Schaink H. M. and Smit J. A. M., *J. Chem. Phys.*, **107** (1997) 1004; Sperry P. R., *J. Colloid Interface Sci.*, **99** (1984) 97; Robb I. D., Williams P. A., Warren P. and Tanaka R., *J. Chem. Soc. Faraday Trans.*, **91** (1995) 3901.
[19] Chatterjee A. P. and Schweizer K. S., *J. Chem. Phys.*, **109** (1998) 10477.
[20] Leung K. and Chandler D., *Phys. Rev. E*, **49** (1994) 2851.
[21] Fabbian L., Götze W., Sciortino F. and Thiery P. T. F, *Phys. Rev. E*, **59** (1999) R1347; Bergenholtz J. and Fuchs M., *Phys. Rev. E*, **59** (1999) 5706.
[22] Kulkarni A. M., Chatterjee A. P., Schweizer K. S. and Zukoski C. F., *Phys. Rev. Lett.*, **83** (1999) 4554; Chatterjee A. P. and Schweizer K. S., *Macromolecules*, **32** (1999) 923.